Simulation of Ultrasonic Propagation in Transformers within Thermal Fields and Intelligent Methodology for Hot-Spot Temperature Recognition

Dongxin He, Dechao Yang, Xinhua Guo, Jiefeng Liu, Haoxin Guo, Qingquan Li, Gilbert Teyssedre

Simulation of Ultrasonic Propagation in Transformers within Thermal Fields and Intelligent Methodology for Hot-spot Temperature Recognition*

Dongxin He[1], *Dechao Yang*[1], *Xinhua Guo*[2], *Jiefeng Liu*[3*], *Haoxin Guo*[1], *Qingquan Li*[1] *and Gilbert Teyssedre*[4]

(1. School of Electrical Engineering, Shandong University, Jinan 250061, China;
2. School of Mechanical and Electronic Engineering, Wuhan University of Technology, Wuhan 430070, China;
3. School of Electrical Engineering, Guangxi University, Guangxi 530004, China;
4. UPS, INPT, CNRS, LAPLACE (Laboratoire Plasma et Conversion d'Energie), University of Toulouse, Toulouse 31100, France)

Abstract: Hot-spot temperature of transformer windings is a crucial indicator of internal defects. However, current methods for measuring the hot-spot temperature of transformers do not apply to those already in operation and suffer from data lag. This study introduces a novel inversion method that combines ultrasonic sensing technology, multiphysics simulation, and the K-nearest neighbors algorithm. Leveraging the penetrative ability and temperature sensitivity of ultrasonic sensing, a detailed physical field simulation model was established. This study extensively investigates the characteristics of ultrasonic wave signals inside transformers. The investigation includes different temperature fields, ranging from 40 ℃ to 110 ℃ at 10 ℃ intervals, and various ultrasonic wave emitter conditions. By extracting the key features of the acoustic signals, such as the peak time, propagation time, and peak amplitude, an accurate inversion of the winding hot-spot temperature is successfully achieved. The results demonstrate that this method achieves a high accuracy rate (98.57%) in inverting the internal winding hot-spot temperatures of transformers, offering an efficient and reliable new approach for measuring winding hot-spot temperatures.

Keywords: Ultrasonic temperature measurement, non-destructive testing, oil-immersed transformers, machine learning

1 Introduction

Oil-immersed transformers are critical components of power systems and play an important role in the conversion and transmission of electrical energy [1-3]. Overloading and failures in the cooling system can result in an increased winding hot-spot temperature, which represents the highest temperature point within the transformer windings [4-6]. An abnormal increase in the winding hot-spot temperature accelerates the aging process of insulation materials, reducing their insulating properties; however, in extreme cases, it can also trigger fires and explosions, posing severe threats to the safety of operational personnel. In addition, such incidents can affect the stable operation of power systems and potentially lead to substantial economic losses. Therefore, it is imperative to implement effective monitoring of the winding hot-spot temperature in transformers during normal operation to prevent accidents and promptly diagnose internal faults [7-9].

Transformer winding temperature measurements involve two main methods: indirect and direct. Indirect methods [10-13] use the top oil temperature and electrical data with a thermal model to estimate winding temperatures. However, these methods may not be accurate owing to complex transformer structures and uneven heat transfer. Direct methods [14-16], such as thermoresistive and fiber-optic

Manuscript received December 15, 2023; revised January 12, 2024; accepted February 1, 2024. Date of publication March 31, 2024; date of current version February 19, 2024.
* Corresponding Author, E-mail: jiefengliu2018@gxu.edu.cn
* Supported by National Natural Science Foundation of China (U1966209, 52277155 and 2021CXGC010210).
Digital Object Identifier: 10.23919/CJEE.2024.000052

sensors, offer higher precision by being placed near or on the windings. Despite their precision, these sensors can be challenging to install and maintain, can distort the temperature field, and are susceptible to harsh conditions, thereby affecting their reliability. Therefore, there is a need for a technology that can monitor internal temperatures without these drawbacks. This study proposes a novel, non-contact, ultrasonic emission-based technique for accurately determining transformer winding hot-spot temperatures, leveraging the ability of ultrasonic technology to provide non-destructive, real-time monitoring with high accuracy and sensitivity.

In recent years, there have been significant advancements and applications of ultrasonic temperature measurement technology. This technology is known for its convenient detection methods, resistance to electromagnetic interference, wide temperature measurement range, and high precision. It has been implemented in various fields, including military, industrial, and agricultural applications [17-18]. For instance, in 2020, John et al. [19] applied an ultrasonic temperature measurement system to a 500 MW coal-fired boiler for utility-scale temperature monitoring and conducted preliminary severity assessments. Additionally, in 2022, Walton et al. [20] developed an ultrasonic method for measuring the spatial distribution of the temperature in solid materials, particularly within extreme process containment ranges.

While ultrasonic temperature measurement technology has yet to see widespread adoption in the transformer sector, ultrasonic testing has demonstrated significant development potential and practical value as an efficient detection method. This technology can identify the deterioration of the insulating materials inside transformers and monitor the structural integrity of the windings. During operation, transformer windings and other critical components may experience minor deformations or damage owing to prolonged thermal, mechanical, or electrical stresses. Through the analysis of ultrasonic signals emitted from these components, ultrasonic testing technology can detect minute changes promptly, thereby preventing potential failures. Li et al. [21] utilized a split-type ultrasonic detection device for online monitoring of changes in transformer windings, guiding the maintenance and repair of electrical equipment. This application for the detection of transformer windings at substations proved the effectiveness and practicality of this device. Moreover, ultrasonic testing technology has been employed for the detection of PDs in transformers [21-22]. Qian et al. [23] proposed a transformer internal positioning method for partial discharge based on GCC-MSSA, allowing for the accurate localization of partial discharges. This facilitates the timely repair or replacement of components, thus ensuring the reliable operation of transformers. These achievements demonstrate the emerging advantages of ultrasonic testing technology in the internal applications of transformers, providing a crucial theoretical basis for the feasibility study of ultrasonics in transformer temperature measurement [24].

Despite the impressive performance of ultrasonic temperature measurement technology in various fields, it faces unique challenges in specific transformer environments. The primary issue is that the existing ultrasonic temperature reconstruction algorithms are not suitable for the complex internal structure of transformers. In these environments, determining the propagation path of ultrasonic waves is difficult due to multiple refractions and reflections. In addition, the composition of multiple components inside the transformers contradicts the assumption of a single medium, thereby increasing the complexity of the measurements.

This study introduces a novel method for hot-spot temperature inversion in transformers, leveraging the synergy between multi-physics simulation technology and artificial intelligence algorithms [25]. We developed a high-fidelity simulation model that accurately represented the heat dynamics of the transformer, including the internal winding heat conduction, oil convection, and air-side convection. By emitting ultrasonic waves into the transformer and analyzing the resulting acoustic pressure distribution, we have investigated how hotspot temperature affects wave propagation. To address challenges such as multiple reflections and complex sound wave paths, we employed an artificial intelligence-based approach using the K-nearest neighbors algorithm (KNN) algorithm. This method analyzes the acoustic signals

from ultrasonic sensors and extracts key features to form a dataset for training and testing. This is an effective diagnostic technique for hot-spot temperatures, allowing for preliminary inversion. This research offers a new non-destructive method for detecting hot-spot temperatures in transformer windings, circumventing the limitations of embedded sensors and presenting advantages over traditional detection technologies.

2 Multiphysical simulation of temperature, fluid dynamics, and acoustic fields in oil-immersed transformers

2.1 Thermal transfer processes within transformers under normal operating conditions

During the operation of transformers, the core and winding losses constitute the primary sources of heat generation within the transformer. Convective heat transfer plays a pivotal role in the heat transfer generated by transformer windings. The internal heat transfer process within the transformer is illustrated in Fig. 1.

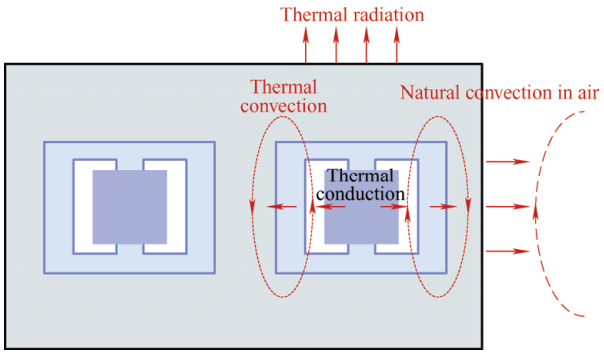

Fig. 1 Heat transfer process in a transformer

In oil-immersed transformers, this heat transfer process primarily occurs at the interface between the windings and the transformer oil. Heat generated by the windings is initially transferred to the transformer oil near the surface of the windings. Within the transformer oil, heated oil molecules rise owing to the decreased density, while cooler molecules sink because of their higher density, forming a convective cycle. This cycle effectively transfers heat from the windings to the oil, and subsequently from the oil to the cooling system or external environment of the transformer. This process conforms to the Navier-Stokes equations

$$\frac{\partial \rho}{\partial t}+\nabla\cdot(\rho u)=0 \tag{1}$$

$$\rho\left(\frac{\partial u}{\partial t}+u\cdot\nabla u\right)=-\nabla p+\nabla\cdot(\mu(\nabla u+(\nabla u)^{\mathrm{T}})-\frac{2}{3}\mu(\nabla\cdot u)\boldsymbol{I})+F \tag{2}$$

$$\rho C\frac{\partial T_{\mathrm{L}}}{\partial t}+\rho Cu\cdot\nabla T_{\mathrm{L}}=\nabla\cdot(k\Delta T_{\mathrm{L}})+Q \tag{3}$$

where t represents time; ρ is the fluid density; u denotes the fluid velocity; p and F correspond to the pressure and volumetric force, respectively; $\boldsymbol{I}$ represents the identity matrix; μ and C represent the fluid dynamic viscosity and specific heat capacity, respectively; T_{L} is the fluid temperature; k is the thermal conductivity coefficient; and Q denotes the heat source.

2.2 Theoretical foundations of ultrasonics

In the field of acoustics, owing to the rapid expansion and compression cycles of the volume element of a medium, heat exchange from outside the volume element is insufficient within these cycles. This renders the propagation of sound waves in an ideal medium an adiabatic process. Building on this theory, our study focuses primarily on the propagation and detection of ultrasonics within transformers under stable temperature field conditions. The propagation of ultrasonic waves inside a transformer through various media is essentially a process in which waves, which vary in space and time, move forward between fluids and solids. Considering the differences between fluids and solids, the transformer model was divided into transformer oil and other regions. This division allows the simulation to emulate the propagation of ultrasonic waves across and between different components.

(1) Wave equation in fluids assuming that transformer oil is a static, homogeneous, and continuous fluid medium, the fundamental equation describing minute acoustic waves in an ideal fluid can be derived from the equations of motion, mass conservation, and state. This results in a three-dimensional wave equation for sound pressure in fluids, as depicted in Eq. (4). This equation reflects the relationship between the instantaneous sound pressure values at various points in the fluid and the values at those points at different times [26].

$$\frac{1}{c_0^2}\frac{\partial^2 \rho}{\partial t^2} - \nabla^2 p = 0 \tag{4}$$

where ρ represents the medium density, p denotes the variation in sound pressure, c_0 is the static speed of sound in the fluid, and ∇^2 is the Laplace operator.

(2) Solid propagation. The characteristics of the ultrasonic wave propagation between solids and liquids differ significantly. The relationship between speed and temperature of solids is complex, making theoretical calculations nearly impossible. However, existing studies suggest that the variation in sound speed with temperature in solids is minimal. Additionally, due to the inherently high speed of sound in solids, this study disregarded the impact of temperature on the ultrasonic wave propagation speed in solids.

(3) Acoustic-solid coupling boundary conditions. To simulate the propagation of ultrasonic waves between fluids and solids, this study employed direct coupling using the structural finite element method and acoustic boundary elements [27]. The boundary conditions were set as follows

$$-n \cdot \left(-\frac{1}{\rho c}(\nabla p_t - q_d) \right) = -n \cdot u_{tt} \tag{5}$$

$$F_A = p_t n \tag{6}$$

where n is the surface normal direction, c is the speed of sound, p_t is the total sound pressure, q_d is the acoustic dipole domain sound source, u_{tt} is the structural acceleration, and F_A is the load acting on the structure.

2.3 Construction of the geometric model

In this study, the modeling was based on a scaled-down experimental model of an actual transformer, with the overall dimensions of the real transformer being 2 350 mm in length, 920 mm in width, and 826 mm in height. Developing a comprehensive simulation model for a transformer is challenging due to the exceptionally complex structure of the actual transformer. Additionally, the modeling of small-sized components is not conducive to mesh division and computational processing. Therefore, to enhance the computational efficiency and accuracy, this study employs a simplified modeling approach. The established simulation model retains only four primary components of the transformer: windings, core, oil tank, and casing. Secondary structures such as bushings and external oil tank systems are disregarded. This simplified model provides accurate simulation results while significantly reducing the simulation computation time and required computational resources, thereby improving the computational efficiency of the simulation outcomes.

The simplified transformer simulation model mainly comprises components such as an oil tank, casing, reinforcing bars, core, and windings. The tank has dimensions of 1.48 m × 0.830 m × 0.732 m with a thickness of 0.01 m and is made of steel material. The reinforcing bars have a D-shaped cross-section, which enhances the strength of the casing. The core, composed of silicon steel, accommodates two sets of high and low voltage windings, constructed from copper and coaxially arranged, with an overall height of 0.45 m. Although the simplified transformer simulation model established in this study makes slight adjustments to the actual internal structure of the transformer, its design and planning approach can provide effective reference and guidance for research and applications in power systems. The overall geometric model of the transformer is illustrated in Fig. 2.

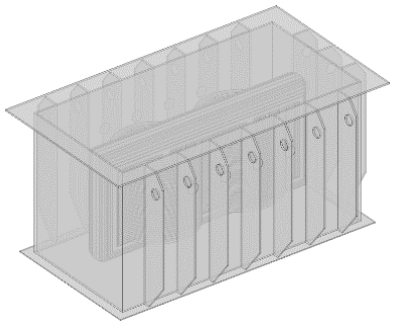

Fig. 2 Geometric model of the transformer

To facilitate the transmission and reception of the ultrasonic signals, 24 ultrasonic sensors were installed on the surface of the transformer. Nine sensors were mounted on the front, six on the sides, and nine were symmetrically distributed on the back. The installation positions of the sensors are illustrated in Fig. 3. Sensors A, B, and C were designated as transmitters,

whereas the others served as receivers of the acoustic signals. Preliminary acoustic tests indicate that when the source signal was a single-cycle signal, the sensors received suboptimal acoustic signals characterized by low amplitude and complex waveforms, making it challenging to discern information such as wave travel time. To enhance the intensity and detectability of the ultrasonic signals, the experiment utilizes a continuous wave of 10 cycles as the source signal with an excitation voltage amplitude of 200 V.

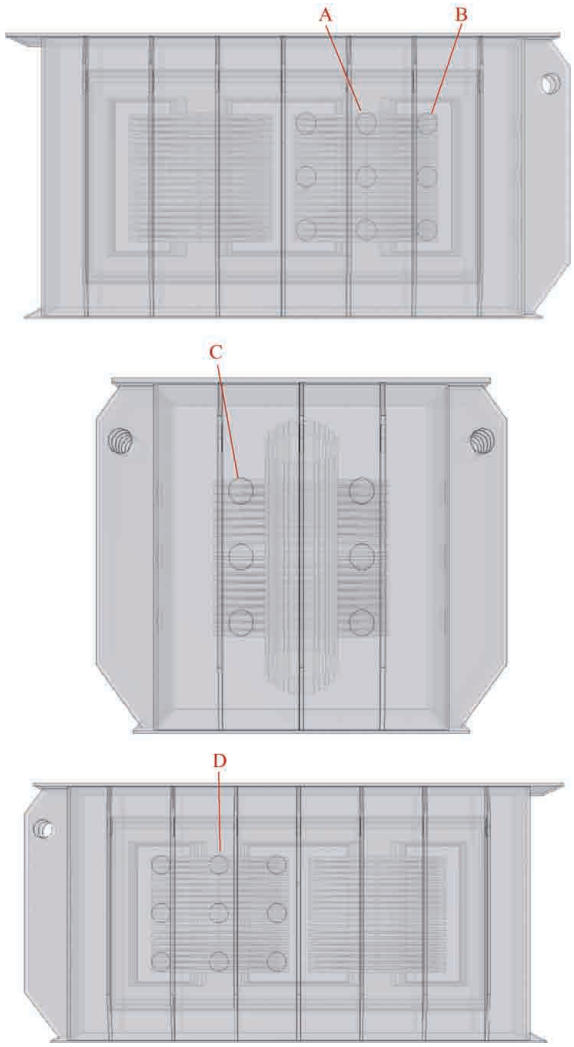

Fig. 3 Sensor arrangement on the transformer surface

3 Simulation results and analysis

3.1 Temperature field distribution in the transformer

The finite element method (FEM) is employed to calculate the thermal-fluid coupled field in the transformer. The environmental temperature is set at 25 ℃, with the external atmospheric pressure at standard atmospheric levels and no wind speed influence. The internal temperature field distributions of the transformer at different power levels were obtained. For example, at a winding power of 4 000 W, the internal temperature field distribution of the transformer is illustrated in Fig. 4.

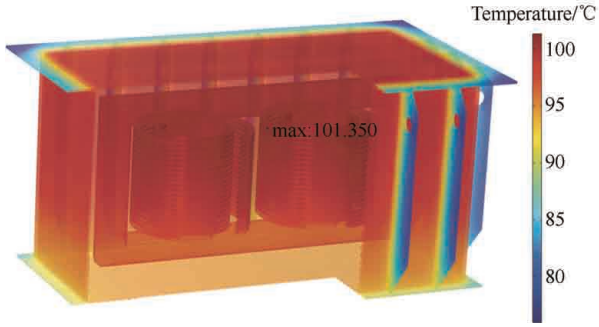

Fig. 4 Temperature field distribution in the transformer

The temperatures of the core and windings are depicted in Fig. 5, demonstrating that the hot-spot temperature of the winding at this time is 101.35 ℃. The hot-spot was located below the top of the winding, specifically at the second coil from the top (i.e., at 91.6% of the axial height of the winding). The overall temperature of the winding exhibited an increasing trend. This is due to thermal convection occurring between the transformer oil and the surrounding heat sources under the influence of temperature gradients. The heated oil expands and becomes denser. Under the effect of thermal buoyancy, it moves upward, continuously exchanging heat with surrounding sources. The continual increase in the oil temperature leads to a reduced temperature difference between the oil and the coils, further diminishing the cooling efficiency of the oil flow. Consequently, the overall temperatures of the windings on both sides exhibited an upward trend. The internal streamline diagram of the transformer is illustrated in Fig. 6.

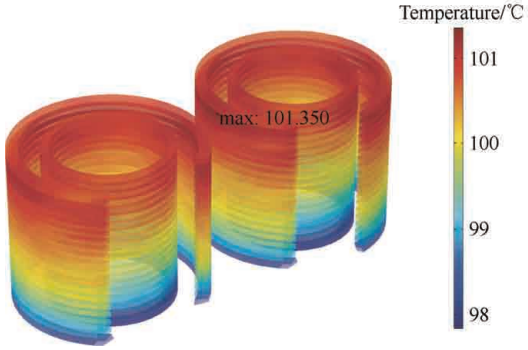

Fig. 5 Temperature distribution of transformer windings

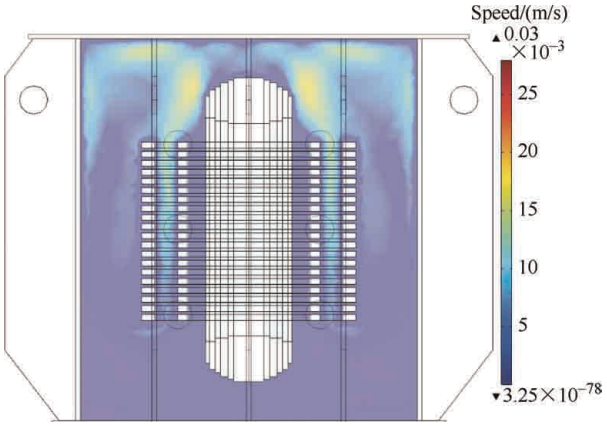

Fig. 6 Temperature distribution of transformer windings

3.2 Acoustic field distribution in the transformer

When the internal temperature field distribution of the transformer is known, ultrasonic signals are emitted inside the casing to obtain the sound pressure distribution as the ultrasonic waves traverse the internal temperature field of the transformer. Considering the emission of the acoustic source signal from Sensor A as an example, the acoustic field distribution under the influence of different hot-spot faults was studied. Setting the initial moment of the sound source signal emission as the zero-time point, Fig. 7 displays the sound pressure distribution when the winding power is 4 000 W, the hot-spot temperature is 101.35 ℃, and the sound wave propagation time of t=0.5 ms.

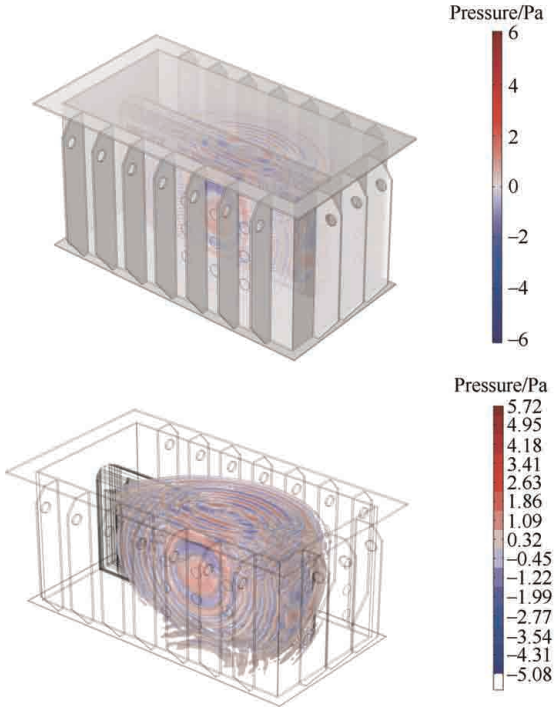

Fig. 7 Acoustic field distribution inside the transformer

Ultrasonic signals emanate from a source and propagate rapidly inside a transformer in the form of spherical waves. As time progresses, ultrasonic waves deviate from regular spherical waves, especially when encountering obstacles such as windings and walls. These encounters result in refraction and reflection, adding complexity to the propagation of acoustic waves inside the transformer. The sound pressure exhibited a ring-like distribution on the surface of the transformer casing. As the sound waves propagate, the isobaric surfaces of the sound pressure alternate and change accordingly.

3.3 Acoustic pressure distribution inside the transformer at different hot-spot temperatures

To further investigate the characteristics of ultrasonic wave transmission inside the transformer under different hot-spot temperature fields, this study analyzed the propagation characteristics of sound waves in various temperature fields using transient sound pressure distribution diagrams simultaneously and from the same emission source cross-section under different temperature conditions, as illustrated in Fig. 8. The hot-spot temperatures are 40 ℃, 60 ℃, 80 ℃, and 100 ℃, with the transient sound pressure distribution diagrams at t=0.2 ms for internal cross-sections A-D. Sensor D is on the back, directly opposite to Sensor A.

As illustrated in Fig. 8, the waveform emitted by the sound source exhibited a certain regularity. As the sound waves spread away from the source, the sound pressure values alternated between positive and negative, with the magnitude of the sound pressure gradually decreasing as the distance from the source increased. Furthermore, by observing the distribution diagrams at these four temperatures, it is noticeable that the diffusion effect of the sound waves weakens as the temperature increases from 40 ℃ to 60 ℃. For instance, focusing on the acoustic field distribution around the high-voltage winding, indicated by the box, it is observed that at the same moment, the sound waves at 40 ℃ propagate farthest from the high-voltage winding, while at 100 ℃, they propagate the shortest distance. The same trend was evident in the sound pressure distribution near the core; the acoustic field distributions became closer as the temperature increased. The side-emission cross-sectional sound pressure distribution is depicted in Fig. 8, which demonstrates that the range of sound wave diffusion

decreased with increasing temperature. These phenomena indicate that the propagation speed of the ultrasonic waves decreased with an increase in the hot-spot temperature field.

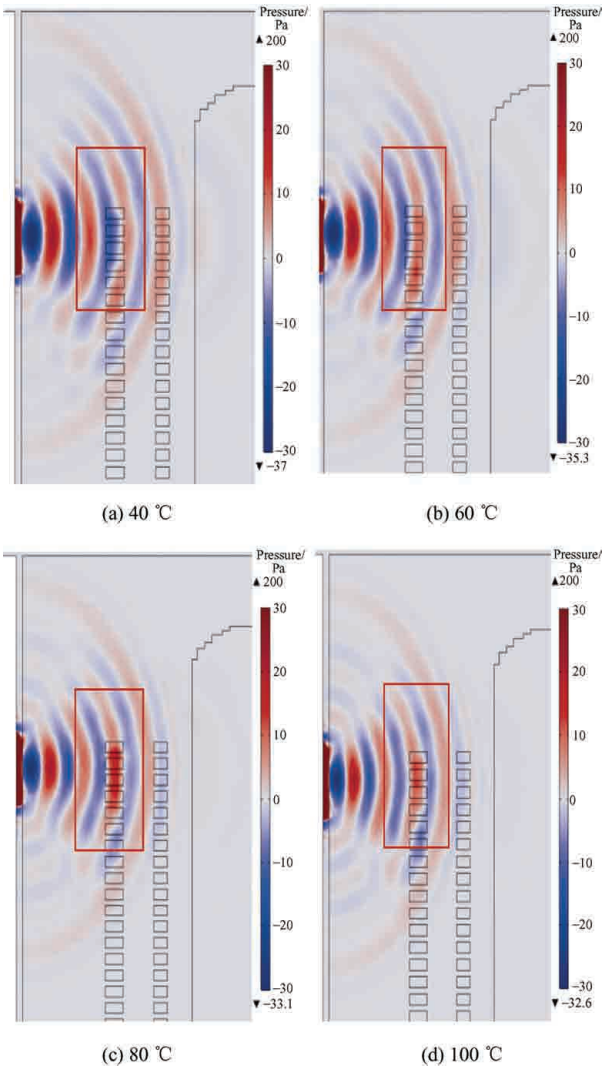

Fig. 8 Internal cross-sectional acoustic pressure distribution in the transformer at t=0.2 ms for temperatures of 40 ℃, 60 ℃, 80 ℃, and 100 ℃

To investigate the impact of temperature on the loss of acoustic wave propagation within transformers, this study compares the sound pressure levels at high-voltage windings when a specific wave peak arrives under different temperature conditions. This approach allows for a more precise quantification of the effect of temperature changes on the propagation loss of sound waves. Consequently, this will deepen our understanding of the dynamic behavior of acoustic waves within transformers under the influence of temperature. Fig. 9 illustrates the sound pressure distribution near the high-voltage windings when a specific wave peak arrives at different hot-spot temperatures.

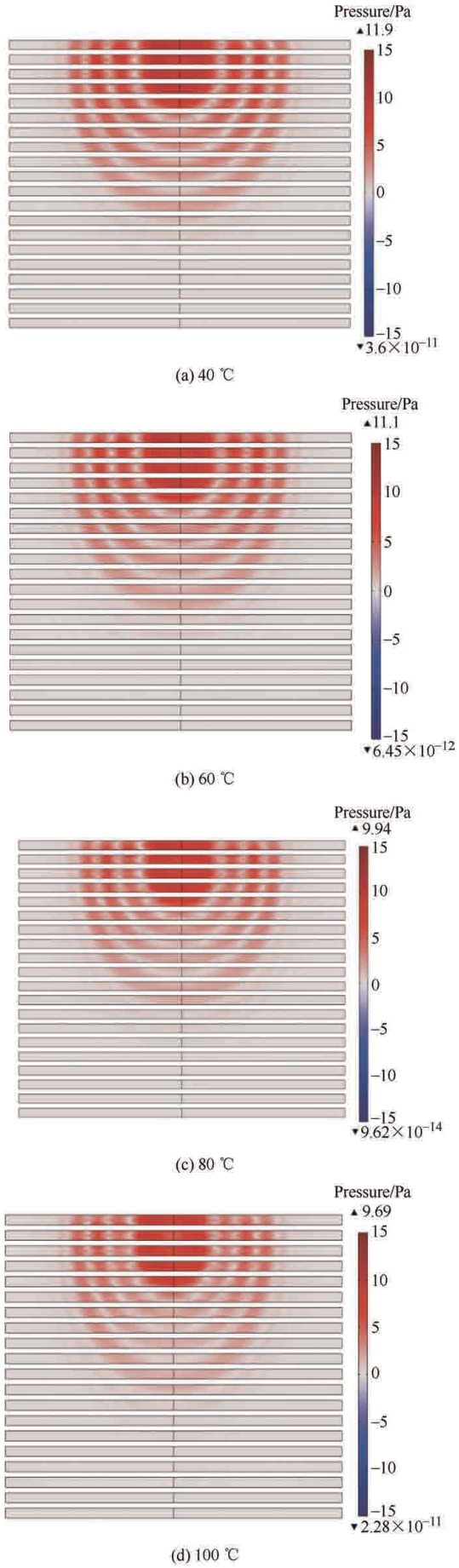

Fig. 9 Absolute acoustic pressure distribution on the transformer surface for the same specific wave peak at different temperatures

The simulation results indicate that as the hot-spot temperature increased from 40 ℃ to 100 ℃ during normal operation, there was a significant change in the maximum value of sound pressure. The absolute maximum sound pressure value changes from 11.9 Pa at 40 ℃ to 11.1 Pa at 60 ℃, then to 9.94 Pa at 80 ℃, and finally to 9.69 Pa at 100 ℃. A detailed comparison of these sound pressure values revealed a clear trend: as the temperature gradually increased, the energy loss of the sound waves during propagation increased, resulting in a lower received sound pressure.

3.4 Changes in received signals at different hot-spot temperatures in the transformer

To further investigate the influence of hot spot temperature rise on ultrasonic wave propagation, this study takes the ultrasonic signals emitted by Sensor A as an example and organizes and compiles the ultrasonic signals collected by other sensors. It is known from the principles of sound wave propagation that, as the propagation time increases, the received sound signals become increasingly complex and indistinguishable owing to repeated refraction and reflection. Therefore, this study focuses on the analysis of ultrasonic signals within a specific time window.

Fig. 10 presents a line graph of ultrasonic wave signals received by Sensor D (directly opposite to Sensor A), emitted at different hot-spot temperatures of 40 ℃, 50 ℃, 60 ℃, 70 ℃, 80 ℃, 90 ℃, 100 ℃, and 110 ℃. The line in Fig. 10a demonstrates that, as the temperature increased, the start time of the signals received by the sensor was progressively delayed, indicating a slower propagation speed of the sound waves within the transformer. The boxed area in Fig. 10b illustrates a sequential decrease in the amplitude of the signals received by the sensor with increasing temperature. This suggests that the internal loss of sound waves in the transformer increases with increasing temperature, and the impact of temperature on the speed of sound wave transmission is also evident.

Fig. 11 illustrates the ultrasonic wave signal curves received by Sensor D, with Sensors B and C emitting signals separately. As the position of the ultrasonic wave emission varied, the loss incurred during transmission also differed. However, the overall trend

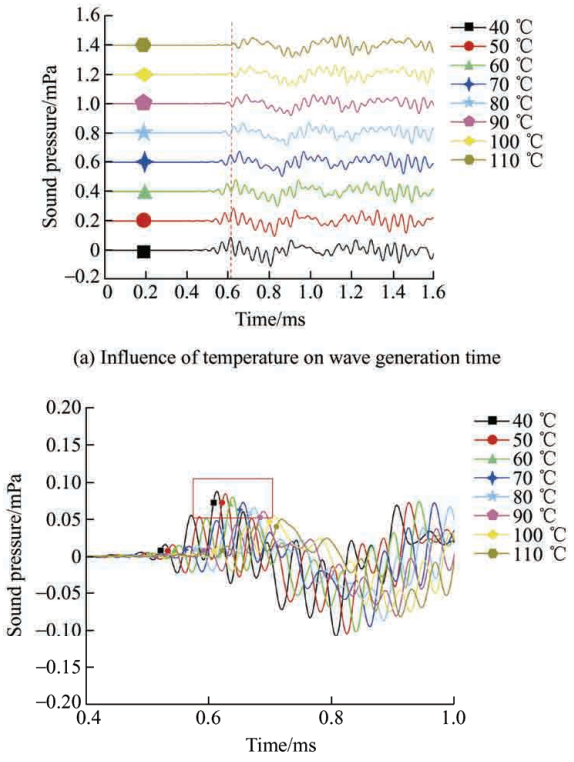

(a) Influence of temperature on wave generation time

(b) Effect of temperature on amplitude

Fig. 10 Signal reception at different temperatures for Sensors A-D

indicates that the amplitude decreases as the temperature increases. As the propagation time of the sound waves increases, the signals become more complex because of repeated refraction and reflection within the transformer, making the characteristic signals less distinct. Therefore, the portion of the waveform signal showing clear amplitude changes in the initial phase of sound wave transmission, specifically between 0.5 ms and 1 ms, is selected as the useful signal. This allows for a more accurate extraction of key information contained in acoustic signals, facilitating subsequent data analysis for classification purposes.

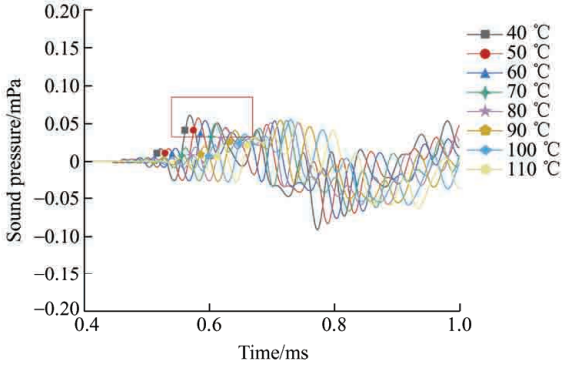

(a) Influence of various temperatures on the amplitude of Sensors B-D

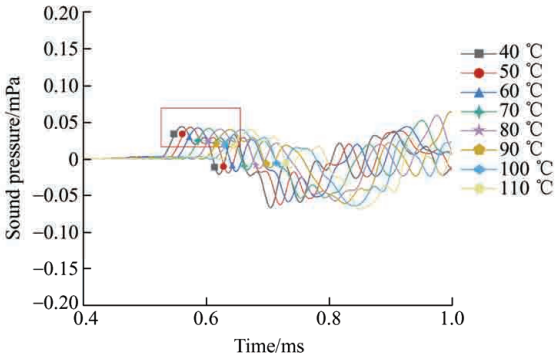

(b) Influence of various temperatures on the amplitude of Sensors C-D

Fig. 11 Signal reception at different temperatures for Sensors B-D and C-D

4 Winding hot-spot temperature inversion based on artificial intelligence algorithms

To meet the practical requirements of temperature measurement, this study consolidated the acoustic signals under different temperature field conditions. Relevant high-correlation feature parameters were extracted from the effective acoustic signals by correlating the impact of the temperature fields on the sound wave propagation. A dataset of acoustic data for hot-spot faults was established, and artificial intelligence algorithms were employed to achieve the inversion of the hot-spot temperature of the transformer.

4.1 Extraction process of feature parameters

In this study, the singular value decomposition (SVD) [28-29] method was utilized to stratify the acoustic signals and successfully extract amplitude change information from the effective acoustic signals. The analysis of these signals involved the extraction of 28 parameters from each signal, such as the peak time, propagation time, and peak amplitude, totaling 1 932 feature parameters. Using Spearman's correlation analysis, 993 feature parameters with high relevance to hot-spot faults were identified and selected.

To further enhance the efficiency and accuracy of data analysis, this study employs principal component analysis (PCA) [30] to extract the most significant 20 principal components from the selected features. The dimensionality reduction offered by the PCA significantly benefits the classification process using the KNN algorithm [31]. The reduced dimensionality of the data facilitates faster processing in KNN classification while simultaneously decreasing the complexity of the feature space, thereby improving the classification accuracy. By eliminating redundant and irrelevant features, the KNN algorithm can recognize and classify acoustic signals more effectively, thus offering a more accurate method for hot-spot fault detection. Thus, the PCA in this study serves not only as a tool for data simplification, but also as a crucial means of enhancing the efficiency and accuracy of acoustic signal classification.

4.2 Construction of the acoustic data set

In the simulation study, to overcome the issue of unique results owing to identical independent variables and to increase the sample size to enhance the classification accuracy of artificial intelligence algorithms, we expanded the temperature range. Building upon the original range of 40 ℃ to 110 ℃, we subdivided each temperature interval, adding temperature points at 0.5 ℃ increments, ultimately forming a temperature sequence starting from 38 ℃ and increasing in 0.5 ℃ steps up to 112 ℃, yielding a total of 72 distinct temperature field samples. This expansion not only enriches the dataset, but also provides more detailed temperature variation information for subsequent analysis. Following the application of principal component analysis (PCA), each sample was condensed into a dataset containing the 20 most crucial principal components. This approach not only enhances the efficiency of data processing, but also improves our understanding and prediction accuracy of the model. Using this method, we can more accurately capture the impact of temperature changes on the characteristics of acoustic signals, thereby providing significant data support for further research on acoustic monitoring and fault diagnosis.

4.3 Hot-spot temperature recognition in windings based on KNN

Owing to their strong nonlinear fitting capabilities, artificial neural network algorithms have become effective methods for equipment fault identification applications in the power sector. In this study, a KNN algorithm was designed to model the mapping relationship between hot-spot temperature information

and the collected signal feature parameters. The KNN is a fundamental and widely used classification and regression algorithm. In classification tasks, the core principle of the KNN algorithm is to identify the K nearest neighbors of a new data point within the training dataset and determine the category of the new point based on the categories of its neighbors. Specifically, the algorithm first calculates the distance between the new data point and each point in the training set and then selects the K closest points. The most frequent category among these selected neighbors was considered the predicted category for the new data point. Thus, the KNN algorithm intuitively and effectively classified new data. A principal diagram of the KNN algorithm is illustrated in Fig. 12.

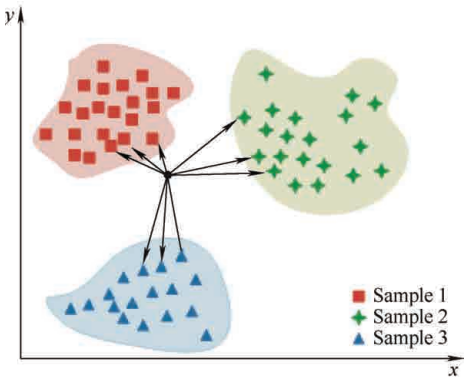

Fig. 12 Principal diagram of the K-nearest neighbor algorithm

In this experiment, the KNN algorithm was employed to analyze the acoustic signals inside the transformer to identify hot-spots at different temperatures. The KNN algorithm determines the category of an unknown sample point based on the most frequent category among its K nearest neighbors. Therefore, the selection of hyperparameter K in the KNN is crucial. Typically, if K is extremely small, the recognition result is highly sensitive to the nearest neighbors and is prone to overfitting; if K is extremely large, the model may be overly influenced by the sample distribution, leading to underfitting. The experiment uses 5-fold cross-validation as the model evaluation method and divides the 72 groups of sample data into training and testing sets. Following multiple rounds of training and testing, the highest recognition accuracy was achieved when K was set to 4, with a temperature classification accuracy of 98.57%. The accuracy curves for different values of K are illustrated in Fig. 13. The confusion matrix for this setting is illustrated in Fig. 14. In addition, the precision, recall, and F1-scores were calculated for K=4, as listed in Tab. 1 provided. Furthermore, it enumerates the specific F1-score values under various temperature conditions, as listed in Tab. 2.

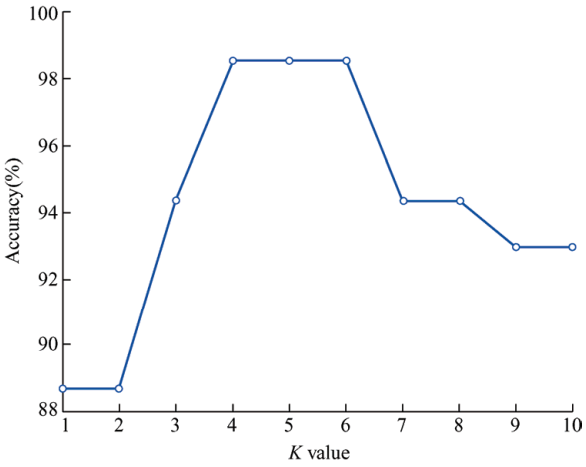

Fig. 13 Effect of K value on accuracy

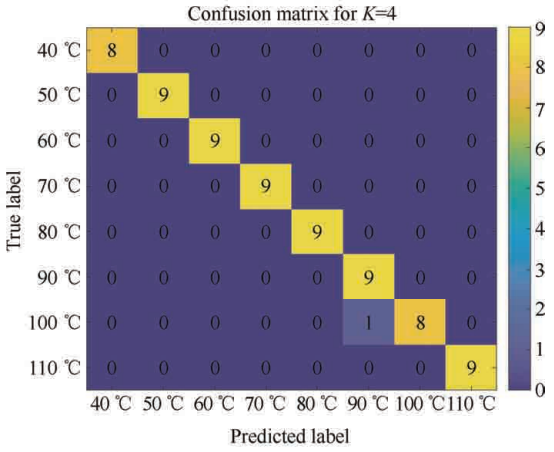

Fig. 14 Confusion matrix for the temperature classification results

Tab. 1 Test results of KNN-based identification models

Evaluation index	Test results(%)
Precision	98.75
Recall	98.63
F1-score	98.63

Tab. 2 F1-score of individual transient

Hot-spot temperature/℃	F1-score(%)
40	100
50	100
60	100
70	100
80	100
90	95
100	94
110	100

This study confirmed that by analyzing the acoustic signals within transformers and utilizing the KNN learning algorithm, it is possible to accurately reflect the impact of temperature changes on sound waves, thereby effectively predicting the hot-spot temperatures of transformer windings. This not only demonstrates the feasibility of the KNN algorithm in practical applications but also provides robust technical support for future transformer health monitoring.

5 Conclusions

This study focuses on a 35 kV oil-immersed transformer and conducts a simulation study on the nondestructive detection of winding hot-spot temperatures based on ultrasonic emission. The propagation characteristics of ultrasonics within the transformer were thoroughly analyzed by constructing a thermal-fluid coupled field and acoustic field simulation model. The effective feature parameters of the ultrasonic signals were successfully extracted and a dataset was constructed based on these parameters. Advanced artificial intelligence algorithms were used to calculate the inversion of the winding hot-spot temperatures. A summary of the research is as follows.

(1) Based on the principles of finite element analysis, a temperature and acoustic field simulation model of a 35 kV transformer was successfully established. Temperature field simulations ranging from 40 ℃ to 110 ℃ were conducted by applying different powers to the windings, followed by detailed simulation studies of ultrasonic wave propagation within the transformer.

(2) This study reveals the significant impact of increasing temperature in the temperature field on the propagation of ultrasonic waves, through in-depth investigation of the sound pressure distribution across transformer sections and absolute total sound pressure distribution on winding surfaces at different temperatures. It was observed that as the temperature increased, the propagation speed of the ultrasonics within the transformer decreased, and the loss during propagation correspondingly increased.

(3) By analyzing sample data under 72 different temperatures, this research delved into the effects of the temperature field on sound wave propagation. The study effectively extracted key feature parameters from acoustic signals. Using the KNN algorithm for data classification, a temperature classification accuracy of 98.57% was achieved, enabling the preliminary inversion calculation of transformer winding hot-spot temperatures.

(4) This simulation study provides a preliminary exploration of ultrasonic temperature measurement techniques within transformers. Future research will be based on these simulation results to conduct ultrasonic temperature measurement experiments on actual transformers and continuously refine the transformer simulation model. By altering the external conditions, such as the environmental temperature, the simulation data will be further enriched. Concurrently, real-world ultrasonic temperature measurement experiments conducted on transformers will be carried out to further validate the simulation data. The integration of the experimental and simulation data aims to achieve a close alignment between the simulated and actual scenarios. In addition, there are plans to employ more efficient artificial intelligence classification algorithms to continually enhance the precision and practical applicability of ultrasonic temperature measurement technology.

References

[1] W Lai, W Li, H Meng, et al. Research on the relation between load coefficient and hot spot temperature of oil-immersed power transformer. *2019 IEEE International Conference on Power*, *Intelligent Computing and Systems (ICPICS)*, Shenyang, China, 2019: 393-396.

[2] J Ruan, Y Deng, Y Quan, et al. Inversion detection of transformer transient hot spot temperature. *IEEE Access*, 2021, 9: 7751-7761.

[3] Y Deng, J Ruan, Y Quan, et al. A method for hot spot temperature prediction of a 10 kV oil-immersed transformer. *IEEE Access*, 2019, 7: 107380-107388.

[4] C Gezegin, O Ozgonenel, H Dirik. A monitoring method for average winding and hot-spot temperatures of single-phase, oil-immersed transformers. *IEEE Transactions on Power Delivery*, 2021, 36(5): 3196-3203.

[5] J Xu, S Liu, Z Li, et al. Modeling and simulation analysis of transformer hot spot temperature based on multi physical field coupling calculation and temperature rise characteristics. *2022 4th Asia Energy and Electrical*

Engineering Symposium (AEEES), Chengdu, China, 2022: 465-471.

[6] S Rong, G Liu, W Wu, et al. Experimental and simulation research on transient temperature distribution of product-level oil-immersed transformer winding. *2020 IEEE International Conference on High Voltage Engineering and Application (ICHVE)*, Beijing, China, 2020: 1-4.

[7] N Saleh, N Azis, J Jasni, et al. Prediction of a transformer's loading and ambient temperature based on SARIMA approach for hot-spot temperature and loss-of-life analyses. *2021 IEEE International Conference on the Properties and Applications of Dielectric Materials (ICPADM)*, Johor Bahru, Malaysia, 2021: 123-126.

[8] Y Luo, L Wang, J Jiang, et al. A method for hot spot temperature monitoring of oil-immersed transformers combining physical simulation and intelligent neural network. *2023 3rd Power System and Green Energy Conference (PSGEC)*, Shanghai, China, 2023: 991-997.

[9] G Liu, Z Zheng, X Ma, et al. Numerical and experimental investigation of temperature distribution for oil-immersed transformer winding based on dimensionless least-squares and upwind finite element method. *IEEE Access*, 2019, 7: 119110-119120.

[10] S Meitei, A Saikia, K Borah, et al. Hot spot detection in high voltage transformer by thermal sensor using COMSOL multiphysics. *2018 2nd International Conference on Power*, *Energy and Environment: Towards Smart Technology (ICEPE)*, Shillong, India, 2018: 1-4.

[11] S Nayyer, J Hozefa, M Rahul, et al. A machine learning perspective in an effective monitoring of thermal performance of transformer. *2023 International Conference on Communication System*, *Computing and IT Applications (CSCITA)*, Mumbai, India, 2023: 209-214.

[12] Z Ni, G Sheng, L Zhang, et al. A dynamic inversion method for hot spot temperature of oil immersed transformers based on a combination of multi physics field simulation and neural network algorithms. *High Voltage Engineering*, 2023, 49(6): 2466-2477.

[13] X Zhang, J Hao, C Liu, et al. Temperature evolution law and identification method of thermal defects in transformer windings. *High Voltage Engineering*: 1-12 [2023-12-15]. https://doi.org/10.13336/j.1003-6520.hve.20230680.

[14] Z Tan. Research on online status monitoring technology for power transformers. *Volkswagen Electric*, 2022, 37(3): 37-39.

[15] M Sahu, S R Sharma, A Singh, et al. An improved infrared thermography technique for hot spot temperature, per unit life and aging accelerating factor computation in transformers. *2020 IEEE International Conference on Computing, Power and Communication Technologies*, Greater Noida, India, 2020: 233-238.

[16] Z Miao, G Jin, J Yang, et al. High temperature area recognition method based on transformer infrared image. *Adhesion*, 2022, 49(12): 125-128.

[17] C Massaroni, A Caponero, R Amato, et al. Fiber Bragg grating measuring system for simultaneous monitoring of temperature and humidity in mechanical ventilation. *Sensors*, 2017, 17(4): 749.

[18] A Finn, K Rogers, J Meade, et al. Spatio-temporal observations of temperature and wind velocity using drone-based acoustic atmospheric tomography. *The Journal of the Acoustical Society of America*, 2019, 145(3): 1903.

[19] M John, K Walton, M Skliar. Ultrasonic measurements of temperature distribution in extreme environments: Results of power plant testing. *2020 IEEE International Ultrasonics Symposium (IUS)*, Las Vegas, NV, USA, 2020: 1-4.

[20] K Walton, M John, M Skliar. Characterization of temperature heterogeneity in utility-scale power plant boilers by spatially distributed ultrasonic measurements. *2022 IEEE International Ultrasonics Symposium (IUS)*, Venice, Italy, 2022: 1-4.

[21] D Li, R Ababaike, G Liu, et al. Application of split type ultrasonic detection device in deformation of power transformer windings. *Transformer*, 2019, 56(12): 64-67.

[22] Z O Prabandaru, R Restianda, R Huda. Determining localization and measuring level of partial discharge in power transformer using acoustic sensor: Case studies at Kemang & Cilegon Baru substation. *2023 4th International Conference on High Voltage Engineering and Power Systems (ICHVEPS)*, Denpasar Bali, Indonesia, 2023: 351-355.

[23] D Qian, K Song, H Xie, et al. Ultrasonic internal positioning method for partial discharge in transformers based on GCC-MSSA. *Electronic Measurement Technology*, 2023, 46(3): 134-141.

[24] C Gao, X Liu. FEM simulation analysis of ultrasonic propagation of partial discharge in transformers. *Power System and Clean Energy*, 2017, 33(10): 14-22.

[25] K Liu, L Guo, B Chen, et al. Analysis of ultrasonic propagation characteristics of partial discharge in oil immersed power transformer. *2020 7th International Forum on Electrical Engineering and Automation (IFEEA)*, Hefei, China, 2020: 66-70.

[26] W Chen, H Xi, X Su, et al. Application of generalized regression neural network in hot spot temperature prediction of transformer windings. *High Voltage Engineering*, 2012, 38(1): 16-21.

[27] L Yu, S Wang, P Wang, et al. Simulation and experimental study on ultrasonic localization of partial discharge in transformer winding. *Insulating Materials*，2019, 52(6): 72-78.

[28] Y Liu, W Tang. De-noising algorithm of AMSVD and its application in PQMD. *Computer Engineering and Applications*, 2016, 52(23): 255-259, 270.

[29] Y Wang, L Zhu. Research and implementation of SVD in machine learning. *2017 IEEE/ACIS 16th International Conference on Computer and Information Science (ICIS)*, Wuhan, China, 2017: 471-475.

[30] H Li, D Xiao. Overview of data-driven fault diagnosis methods. *Control and Decision*, 2011, 26(1): 1-9, 16.

[31] Y Sang. Research on classification algorithm based on K-nearest neighbors. Chongqing: Chongqing University, 2009.

Dongxin He received the B.S. degree in Electrical Engineering from Shandong University and a Ph.D. degree from North China Electric Power University in Beijing. In 2015, he travelled to the LAPLACE Laboratory at the University of Toulouse, France, as a Visiting Scholar. He is currently an Associate Professor at Shandong University, Jinan, China. His research interests include space-charge characteristics in insulation materials, such as cable insulation and power device encapsulation insulation. He has been selected for the Young Talent Lifting Project of the China Association for Science and Technology (CAST).

Dechao Yang was born in the Hebei Province, China. He received the B.S. degree from Shandong University, Shandong, China, in 2023. He is currently pursuing a Master's degree in Electrical Engineering at Shandong University, Shandong, China. His current research interests are primarily focused on the use of ultrasonic sensing technology combined with multiphysics simulations to investigate and analyze hotspot temperatures inside converter transformers.

Xinhua Guo received his Ph.D. in Information Processing from the Tokyo Institute of Technology, Tokyo, Japan, in 2014. From May 2014 to September 2016, he served as an Assistant Professor at the School of Mechanical and Electronic Engineering, Wuhan University of Technology, China. He has been an Associate Professor since October 2016. His research interests include acoustic sensing, imaging, and control methods.

Jiefeng Liu was born in Hebei, China in 1985. He received his M.S. and Ph.D. degrees in Electrical Engineering from Chongqing University, Chongqing, China in 2011 and 2015, respectively. In 2018, he joined Guangxi University, where he serves as an Associate Professor at the School of Electrical Engineering. He has authored and co-authored over 90 papers published in journals and conferences. Dr. Liu's research interests include insulation condition assessment and fault diagnosis of transformers.

Haoxin Guo was born in Yantai, China. He received his B.S. degree from Qingdao University, Qingdao, China in 2022. Currently, he is pursuing his Master's degree in Electrical Engineering at Shandong University, Shandong, China. His research interests focus on machine learning algorithms for monitoring internal hot spot temperatures in converter transformers based on ultrasonic thermometry.

Qingquan Li was born in Laiwu city, Shandong Province, China, in 1969. He received the Ph.D. degree in Electrical Engineering from Xi'an Jiaotong University, Xi'an, China, in 2003. Currently, he is a Professor at Shandong University, Jinan, China. His research interests include the lightning protection and grounding technology, the high voltage insulation and measurement technology, and the detection and diagnosis techniques for electrical equipment.

Gilbert Teyssedre was born in May 1966 in Rodez, France. He received his Engineer degree in Materials Physics and graduated in Solid State Physics in 1989 at the National Institute for Applied Science (INSA). Then he joined the Solid State Physics Lab in Toulouse and obtained his Ph.D. degree in 1993 for work on ferroelectric polymers. He entered the CNRS in 1995 and has been working since then at the Electrical Engineering Lab (now LAPLACE) in Toulouse. His research activities concern the development of luminescence techniques in insulating polymers with focus on chemical and physical structure, degradation phenomena, space charge and transport properties. He is currently Research Director at CNRS and is leading a team working on the reliability of dielectrics in electrical equipment.